Research Paper

Construction and validation of an immunoediting-based optimized neoantigen load (ioTNL) model to predict the response and prognosis of immune checkpoint therapy in various cancers

Xiaofan Su[1,2,3,*], Haoxuan Jin[2,3,*], Jiaqian Wang[2,3,*], Huiping Lu[2,3], Tiantian Gu[2,3], Zhibo Gao[2,3], Manxiang Li[1]

[1]Department of Respiratory and Critical Care Medicine, The First Affiliated Hospital of Xi'an Jiaotong University, Xi'an, Shanxi 710061, China
[2]YuceNeo Technology Co., Ltd., Shenzhen 518000, China
[3]YuceBio Technology Co., Ltd., Shenzhen 518020, China
[*]Equal contribution

Correspondence to: Zhibo Gao, Manxiang Li; **email:** gaozhb@yucebio.com, manxiangli@xjtu.edu.cn
Keywords: neoantigen, immunoediting, checkpoint inhibitors, response, prognosis
Received: December 28, 2021 **Accepted:** April 12, 2022 **Published:** May 25, 2022

ABSTRACT

Background: Only a minority of patients clinically benefit from immune checkpoint therapy. Tumor clones with neoantigens have immunogenicity; therefore, they are eliminated by T-cell-mediated immune editing. Identifying neoantigen clones with the ability to induce immune elimination may better predict the clinical outcome of immunotherapy.

Methods: We developed ioTNL model, which indicates the immunoediting-based optimized tumor neoantigen load, by identifying tumor clones that could induce immune elimination. Data of more than two hundred patients from our patient pool and previously reported studies who underwent anti-PD-(L)1 therapy were collected to validate the prediction performance of ioTNL model. Clonal architectures, immune editing scores and ioTNL scores were identified. The association between the response as well as prognosis and the ioTNL were evaluated. Panel sequencing of genes from 2,469 patients within 20 cancer types was performed to profile the landscape of immunoediting.

Results: As expected, the ioTNL score could predict the response in patients who underwent immune checkpoint inhibitor (ICI) immunotherapy for various cancers, including non-small cell lung cancer (NSCLC; p = 0.0066), skin cutaneous melanoma (SKCM; p = 0.026) and nasopharyngeal carcinoma (NPC; p = 0.0025). Patients with a high ioTNL score demonstrated longer survival than those with a low score. We verified the ioTNL on our cohort through panel sequencing and found that the ioTNL was associated with the response (p = 0.025) and prognosis (p = 0.00082) in anti-PD-(L)1 monotherapy. In addition, we found that the immune editing score correlated with the tumor mutation burden (TMB) and the objective response rate of immunotherapy.

Conclusions: Identifying neoantigen clones with the ability to induce immune elimination would better predict the efficacy of immunotherapy. We have proved that the reliable method of ioTNL can be applied to whole-exome sequencing (WES) and panel data and would have a broad application in precision diagnosis in immunotherapy.

INTRODUCTION

Although immunotherapy using checkpoint inhibitors has significantly improved the overall survival of patients in many malignancies, only a minority of patients achieve benefits [1]. The challenge in predicting the efficacy of checkpoint inhibitors using biomarkers is far from being solved. Checkpoint inhibitors induce tumor elimination by exploiting T cell responses to tumor antigens. Neoantigens, a type of tumor-specific antigens derived from non-silent mutations, are presented by major histocompatibility complex (MHC) molecules and then recognised by T-cell receptors (TCR) as "non-self" peptides.

Several recent studies have revealed that neoantigens are an important factor in determining the response to checkpoint inhibitors [2, 3]. The neoantigen load, which is the sum of putative neoantigens, has been identified as a predictive biomarker in patients treated with checkpoint inhibitors in several clinical cohorts. A disadvantage of assessing the traditional neoantigen load is that different neoantigens are treated equally, although their characteristics are complicated in tumors. Neoantigens derived from truncal mutations were reported to have higher immunogenicity and correlated more with the response than those from non-truncal mutations [2]. The heterogeneity of neoantigens might influence immune surveillance, thereby mediating tumor evolution [4]. A fitness model constructed based on the evolutionary theory of neoantigens proved its ability to predict the efficacy of immunotherapy [3]. For each tumor clone, it is believed that a small set of high-quality neoantigens with high binding affinity to the MHC and TCR, rather than all the putative neoantigens, is sufficient to induce a T-cell response.

A recent study reported that neoantigens could direct immune escape through multiple immunoediting mechanisms under immune selection pressure [2]. Reduced numbers of neoantigens were observed due to a decrease of neoantigen expression or deletion of chromosomal regions containing truncal alterations, thus resulting in immune escape [5, 6]. In some cases, the tumor might lose the heterozygosity of HLA genes or decrease the expression of genes in the neoantigen presentation pathway as an immune escape mechanism [7, 8]. These reports lead to a hypothesis that only the tumor clones with immune elimination capability can be recognised and eliminated by T cells, while immune-edited tumor clones would acquire immune escape from administration. Therefore, patients with a high neoantigen concentration in clones that show immune elimination capability might respond better to immunotherapy.

In this study, we developed an ioTNL score for quantitative characterisation of the neoantigen concentration with immune elimination capability at the patient level to predict the clinical outcome of immunotherapy. We included five cohorts treated with checkpoint inhibitors to investigate the relationship between the ioTNL and patient response or survival (Supplementary Table 1). Our work proved that the ioTNL could predict the clinical outcome following treatment with checkpoint inhibitors. Immunoediting is a relevant predictor of neoantigen immunogenicity that can be considered while selecting neoantigen targets for adoptive cell transfer and vaccine studies.

RESULTS

Constructing the neoantigen quantitative model with immune elimination capability

We developed ioTNL, an algorithm model that evaluates the concentration of neoantigens in tumor clones with immune elimination capability (Supplementary Figure 1). If a tumor clone acquired immune escape and tolerance to immunoediting neoantigens, it would not contribute to the tumor immunogenicity and would be discarded while calculating the neoantigen load. Only the tumor clones with immune clearance ability would be retained (Figure 1A). The calculation of the ioTNL comprises several steps. First, the cluster of each tumor clone is identified based on the allele frequency and corresponding ploidy of the detected mutations. Second, the immune editing score of each clone is calculated. The tumor was heterogeneous with different clones, and the immune stages of clones were various. We used the ratio of the neoantigen to non-silent mutation to calculate the immune editing score. A tumor clone with a high immune editing score was considered to be in the immune escape stage, otherwise, in the immune elimination stage. Subsequently, the neoantigen load indexes of the immune elimination clones were estimated. Neoantigens are identified as 8 to 11 amino acids for class I MHC-binding peptides, which arise from non-silent mutations. A previous study reported that insertions and deletions (InDels) generate a higher number of neoantigens than missense mutations. Based on the hypothesis that InDel mutations may be more immunogenic than missense mutations, neoantigens derived from InDels were also included in the ioTNL model [9]. Therefore, the design of the ioTNL model is consistent with the idea that truncal neoantigens in clonal have higher immunogenicity and correlated more with the response than subclonal neoantigens [2]. Finally, the sum of the cancer cell fraction of each neoantigen in the immune elimination clones was calculated as the ioTNL score.

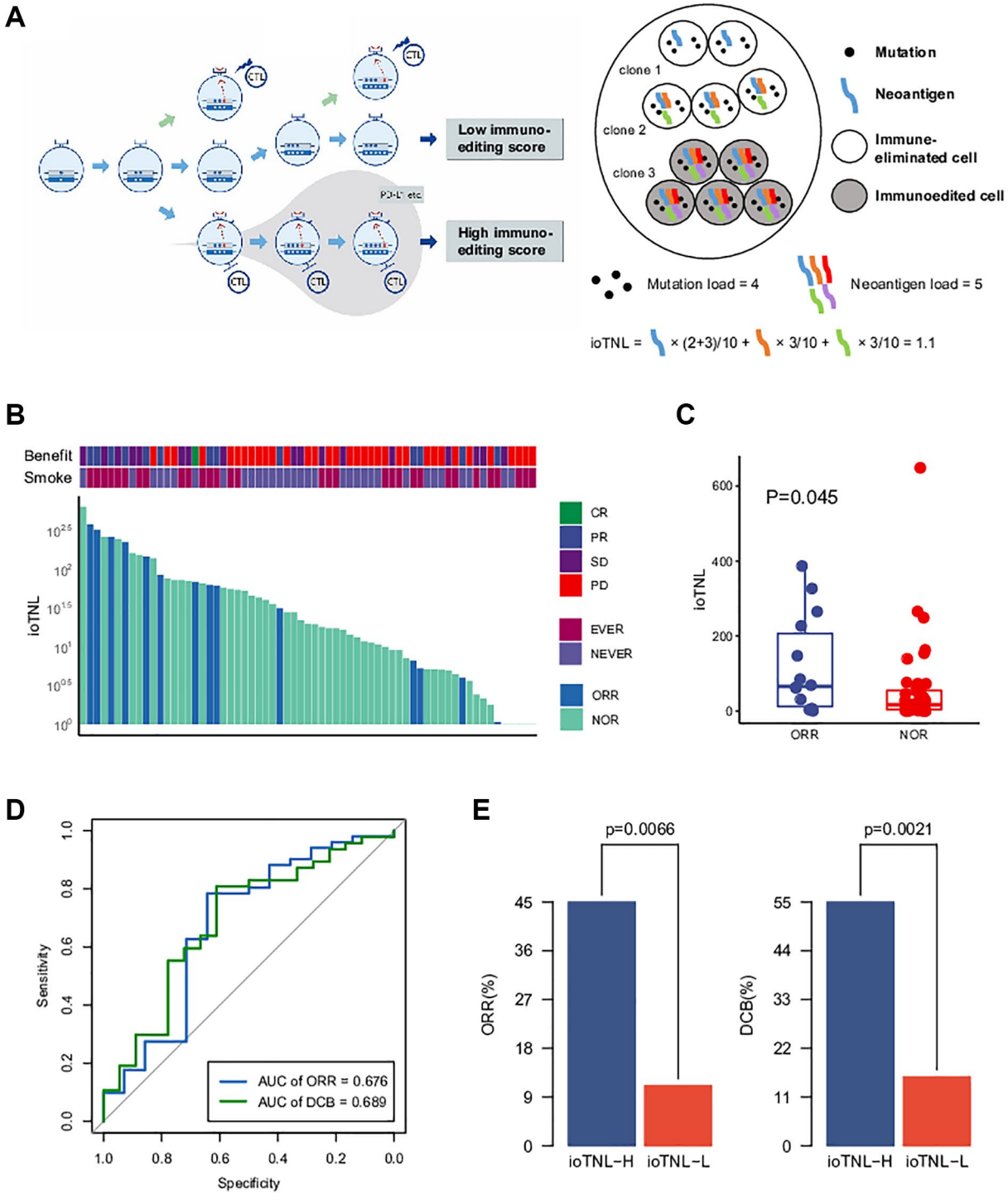

Figure 1. The model of immunoediting-based optimized neoantigen load (ioTNL). (**A**) Illustration showing the concept of ioTNL model. Left, due to the instability of the genome, the tumor produces different clones. If tumor clones acquired immune escape and immune tolerance to neoantigens, they would not contribute to the tumor immunogenicity and would be discarded. Only the tumor clones with immune clearance ability would be retained. Right, we demonstrated a hypothetical tumor of three clones. Tumor cells from clone 1 and clone 2 were immune-eliminated cells while tumor cells from clone 3 were immunoedited cells. We assumed that this tumor had five neoantigens so that the tumor neoantigen load was equal to 5. However, neoantigens from immunoedited cells were excluded so that the ioTNL score of this tumor was equal to 1.1. (**B**) Distribution of ioTNL score in the NSCLC cohort. Patients with objective response (ORR) were labeled in blue while patients with non-objective response (NOR) were labeled in cyan. The scores of ioTNL were transformed into log10 format. (**C**) Boxplot of the distribution of ioTNL scores between patients with ORR and NOR. (**D**) Sensitivity and specificity of ioTNL in predicting ORR and DCB in NSCLC cohort. (**E**) Barplots of ORR rate (left) and DCB rate (right) between ioTNL-H group and ioTNL-L group.

Better response to checkpoint inhibitors is associated with higher ioTNL in multiple cancers

To investigate the implications of the ioTNL in the response to checkpoint inhibitor treatment, we considered a non-small cell lung cancer (NSCLC) cohort from the study by Fang et al. [10]. The cohort included 65 patients who were treated with second-line anti-PD-1/PD-L1 therapy. Previous studies revealed that the tumor mutation burden (TMB) was associated by whole-exome sequencing (WES), and the ioTNL score of each patient was calculated (Supplementary Table 2, Figure 1B). We found that patients with an objective response rate (ORR; [CR/PR]) had significantly higher ioTNL than those with a no objective response (NOR, SD/PD; p = 0.045, Figure 1C), as well as in a durable clinical benefit (DCB, p = 0.019, Supplementary Figure 2A). The ROC curve showed that the AUCs were 0.676 and 0.689 in predicting the ORR and DCB, respectively (Figure 1D). Patients were divided into ioTNL high and low groups based on the Youden index (the maximum sensitivity and the best specificity under the AUC curve). Patients with high ioTNL had a higher ORR (45% vs. 11%, p = 0.007) and DCB (55% vs. 15.6%, p = 0.002) than those with low ioTNL (Figure 1E).

We analysed three more clinical cohorts of different cancer types treated with immune checkpoint inhibitors (ICIs) to further validate the prediction efficacy of the ioTNL. The three cohorts were a skin cutaneous melanoma (SKCM) cohort of 64 patients who underwent nivolumab treatment (Riaz et al.), [11] an intrahepatic cholangiocarcinoma (ICC) cohort of 17 patients (Feng et al.) [12] and a nasopharyngeal carcinoma (NPC) cohort of 61 patients (Fang et al.) [13] The ioTNL scores of 33 patients who received nivolumab as the second-line therapy were evaluated in the SKCM cohort (Supplementary Table 3). A relatively higher median ioTNL score was observed in patients who achieved an ORR (p = 0.058, Figure 2A, left).

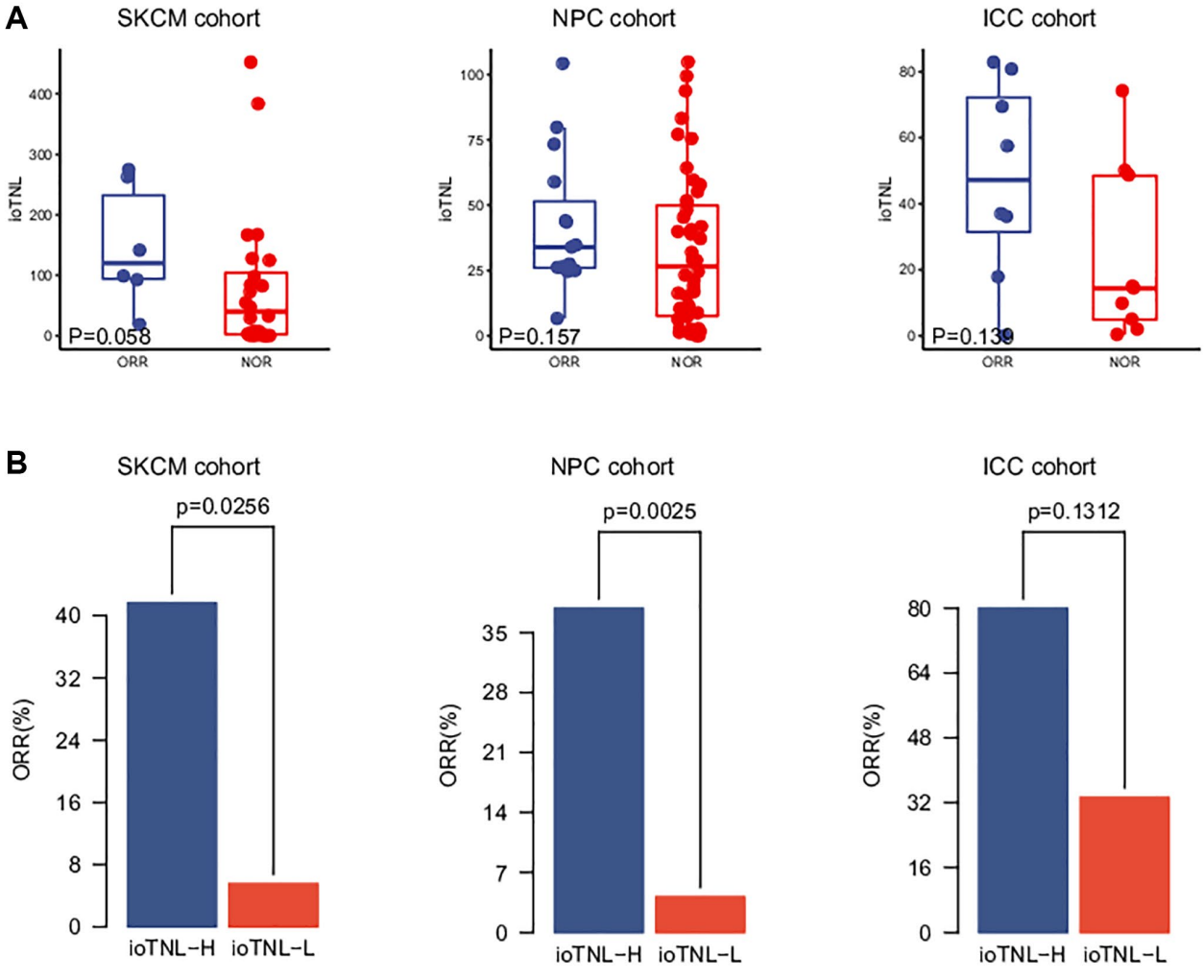

Figure 2. Validation of ioTNL in multiple datasets. (**A**) Boxplots of the distribution of ioTNL scores between patients with ORR and NOR in the SKCM cohort (left), the NPC cohort (middle) and the ICC cohort (right). (**B**) Barplots of ORR rate between ioTNL-H group and ioTNL-L group in the SKCM cohort (left), the NPC cohort (middle) and the ICC cohort (right).

Moreover, patients in the ioTNL-high group, determined by the Youden index described above, had a significant ORR (41.7% vs. 5.6%, p = 0.0256, Figure 2B, left) compared with those in the ioTNL-low group. A similar result was achieved in the second validation cohort of 61 patients with advanced NPC who received anti-PD-1 therapy alone or in combination with chemotherapy. In contrast to most anti-PD-1-responsive solid tumors, NPC has a modest mutation burden (Supplementary Table 4). Patients with a high ioTNL had a significantly better ORR (p = 0.0025, Figure 2B, middle) and DCB (p = 0.008, Supplementary Figure 2B). Furthermore, we collected the data of 17 patients with ICC who received the combination of nivolumab and chemotherapy (Supplementary Table 5). Patients who achieved CR or PR showed a tendency of higher ioTNL than those who did not (p = 0.139, Figure 2A, right); however, the tendency was not significant due to the small cohort size. In addition, patients in the ioTNL-high group demonstrated a higher ORR than those in the ioTNL-low group (80% vs. 33.3%, p = 0.131, Figure 2B, right).

Higher ioTNL predicts a more favourable prognosis in multiple cancers

We examined the association between the ioTNL and prognosis in the NSCLC, SKCM, NPC and ICC cohorts to understand the implications of immunoediting heterogeneity on patient survival. We speculated that patients with a low immune editing score, the neoantigens in which were considered to be in the immune elimination stage, are more likely to benefit from checkpoint inhibitor therapy. As expected, we observed that higher ioTNL scores had a significantly positive association with better survival in these patients. In the NSCLC cohort, progression-free survival (PFS) in patients with a high ioTNL was longer than in those with a low ioTNL (median 161 days vs. 61 days, P < 0.001, Figure 3A). In the melanoma cohort, the overall survival (OS) was prolonged (p = 0.011, Figure 3B) in patients with a high ioTNL than in those with a low ioTNL. Analysis of the NPC cohort also indicated that the OS was significantly longer in the ioTNL-high than in the ioTNL-low group (median 105

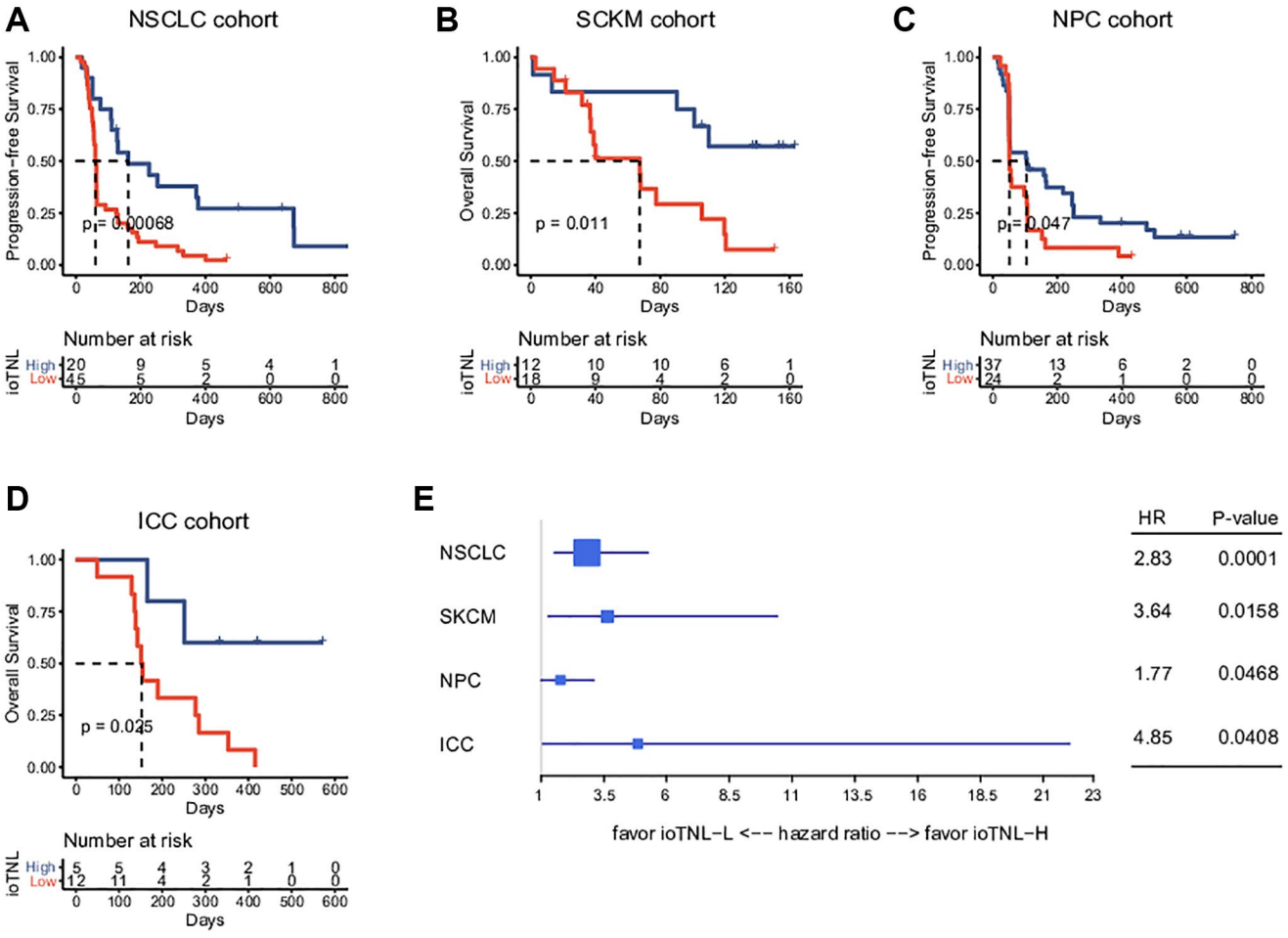

Figure 3. Prognosis analysis of ioTNL in multiple datasets. Kaplan-Meier estimator was used to visualize the survival of ioTNL-H group and ioTNL-L group in the NSCLC cohort (**A**), the SKCM cohort (**B**), the NPC cohort (**C**) and the ICC cohort (**D**). (**E**) Forest plot for the hazard ratios of ioTNL in four cohorts. Larger boxes indicate statistical significance.

days vs. 52.5 days, $p = 0.047$, Figure 3C). Analysis of the ICC cohort revealed a longer PFS among patients in the ioTNL-high group ($p = 0.025$, Figure 3D). The hazard ratios of above four datasets revealed high ioTNL level was a positive factor for prognosis (Figure 3E).

Association between the ioTNL score and other immunotherapy biomarkers

We analysed the association between TMB as well as TNL and clinical outcomes to compare the predictive performance of ioTNL with known genomic biomarkers of immunotherapy (Supplementary Figure 3). The TMB could significantly predict response only in the NSCLC cohort ($p = 0.01$, Supplementary Figure 3A, left). Similarly, TNL could also predict response only in the NSCLC cohort ($p = 0.0475$, Supplementary Figure 3A, right). In the other three cohorts, patients with a high TMB or a high TNL had a tendency of better response; however, the outcomes were not significant (Supplementary Figure 3B–3D). We used the ROC curve to measure the predictive efficiency in the four cohorts. We found that the AUC of the ioTNL was greater than that of the TMB and TNL in all four cohorts (Figure 4A–4D, left). Following this, the association between the TMB as well as TNL and survival were analyzed. TMB could predict survival in two cohorts, namely, NSCLC ($P < 0.001$, Figure 4A, middle) and SKCM ($p = 0.027$, Figure 4B, middle). Similarly, TNL could predict survival in the NSCLC ($p = 0.0037$, Figure 4A, right) and the SKCM cohorts ($p = 0.03$, Figure 4B, right). However, the ioTNL could predict survival in all four cohorts and had more significant p values (Figure 3A–3D). The association between biomarkers of the microenvironment and the ioTNL was compared in the SKCM cohort. Immune checkpoint genes (PD-1, PD-L1 and CTLA4), immune cell abundance (CD8+ T cell and CD4+ T cell) as well as immune signatures (cytolytic, IFN-gamma and T cell exhaustion signatures) were identified from RNA transcriptome data. None of these microenvironment biomarkers correlated with the ioTNL (Spearman correlation <0.2, Figure 4E). Taken together, our data demonstrated that the ioTNL is a better genomic biomarker than the TMB and TNL in predicting the efficacy of immunotherapy. In addition, the ioTNL is independent of the microenvironment biomarkers.

Panel-based immune editing score correlated with the TMB and ORR of immunotherapy in different cancers

Compared with WES, target sequencing on an appropriate region size of the panel would be a cost-effective alternative for clinical detection. To facilitate the application of immunoediting status to clinical detection and the assessment of the ioTNL, we designed YuceOne, a 1.4M panel assembled by screening genomic regions and HLA genes that are susceptible to neoantigens. We collected the data of 2,469 patients across 20 cancer types and applied them on YuceOne to detect mutations and predict neoantigens (Supplementary Table 6). The same approach was followed to calculate the immune editing scores in each clone cluster for each patient. We demonstrated the landscape of immune editing scores across 20 cancer types and found that the majority of the clones had scores ranging from 0 to 10, with a median value of approximately 1 (Figure 5A). Carcinomas such as LUSC, SKCM, PRAD, BLCA and STAD had lower median immune editing scores than 1, implying stronger immune clearance in the clones. On the other hand, carcinomas such as SARC, LIHC and THYM had higher median immune editing scores than 1, implying more severe immune escape in the clones (Figure 5A).

A previous study reported a significant correlation between the median TMB and the ORR following anti–PD-(L)1 therapy [1]. To explore whether the immune editing score has a similar correlation with the TMB and ORR, we collected the median TMB and response data of ICI monotherapy for each cancer type. We plotted the median TMB and the ORR for anti–PD-(L)1 therapy against the corresponding median immune editing score across multiple cancer types (Supplementary Table 7). There was a significant negative correlation between the immune editing score and the TMB ($R = -0.54$, $p = 0.014$, Supplementary Figure 4A). Carcinomas with a high TMB such as SKCM, LUSC and BLCA had lower median immune editing scores, indicating stronger immune clearance in the tumor clones. We also observed a similar tendency of negative correlation between the immune editing score and clinical response; however, the outcomes were not significant ($R = -0.45$, $p = 0.12$, Supplementary Figure 4B). The lower the median immune editing score in one cancer type, the higher the ORR for its anti–PD-(L)1 therapy.

ioTNL identified by the target panel predicted the clinical outcome of immunotherapy

The datasets used for evaluating and verifying the ioTNL were derived from WES. To expand the application of the ioTNL model and explore whether it can predict the response to immunotherapy on a panel level, we collected the data of 21 patients with NSCLC with complete clinical outcomes who underwent anti-

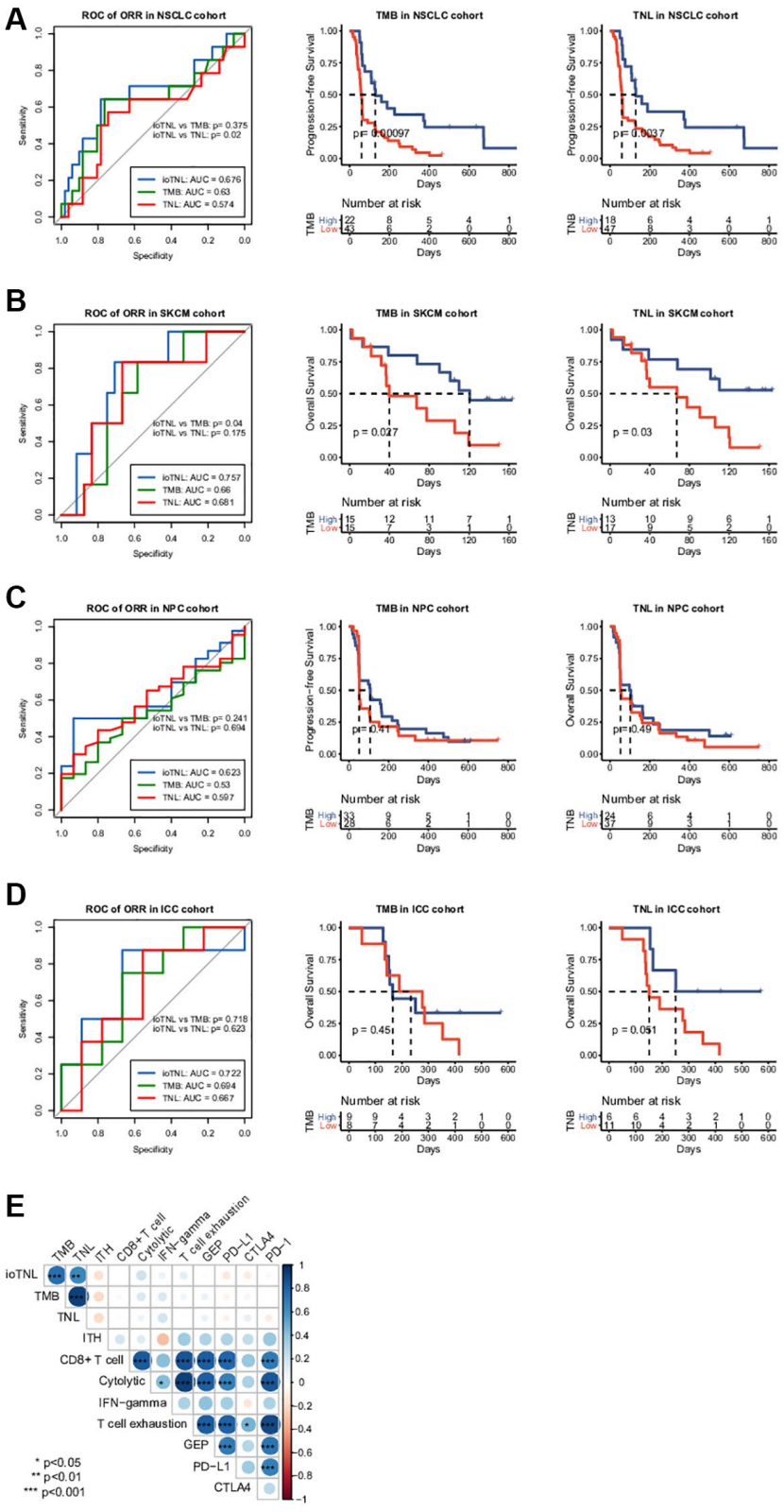

Figure 4. Association between ioTNL score and other immunotherapy biomarkers. Comparison of the response prediction among TMB, TNL and ioTNL in the NSCLC cohort (**A**, left), the SKCM cohort (**B**, left), the NPC cohort (**C**, left) and the ICC cohort (**D**, left). Kaplan-Meier analysis of patient survival of TMB and TNL in the NSCLC cohort (**A**, middle and right), the SKCM cohort (**B**, middle and right), the NPC cohort (**C**, middle and right) and the ICC cohort (**D**, middle and right). (**E**) Spearman correlation of ioTNL with genomic biomarkers and microenvironment-related biomarkers in SKCM cohort. Positive correlations are labeled in blue and negative correlation are labeled in red. Size of circle represented the value of correlation.

PD-1/PD-L1 therapy and identified the ioTNL using YuceOne. Consistent with the previously reported findings, the ioTNL scores could successfully predict the response to immunotherapy (Supplementary Table 8). Patients with a DCB and ORR showed a higher ioTNL (Figure 5B). Patients in the ioTNL-high group, had a significant DCB (100% vs. 21%, p = 0.001, Figure 5C) and ORR (57% vs. 7%, p = 0.025, Figure 5D) compared with those in the ioTNL-low group. Meanwhile, PFS analysis revealed that patients with higher ioTNL had a longer survival time (P < 0.001, Figure 5D). For comparison, the TMB and TNL were also evaluated in our cohort (Supplementary Table 2), and the ROC curves showed that the ioTNL performed better in predicting the response to immunotherapy (Figure 5E).

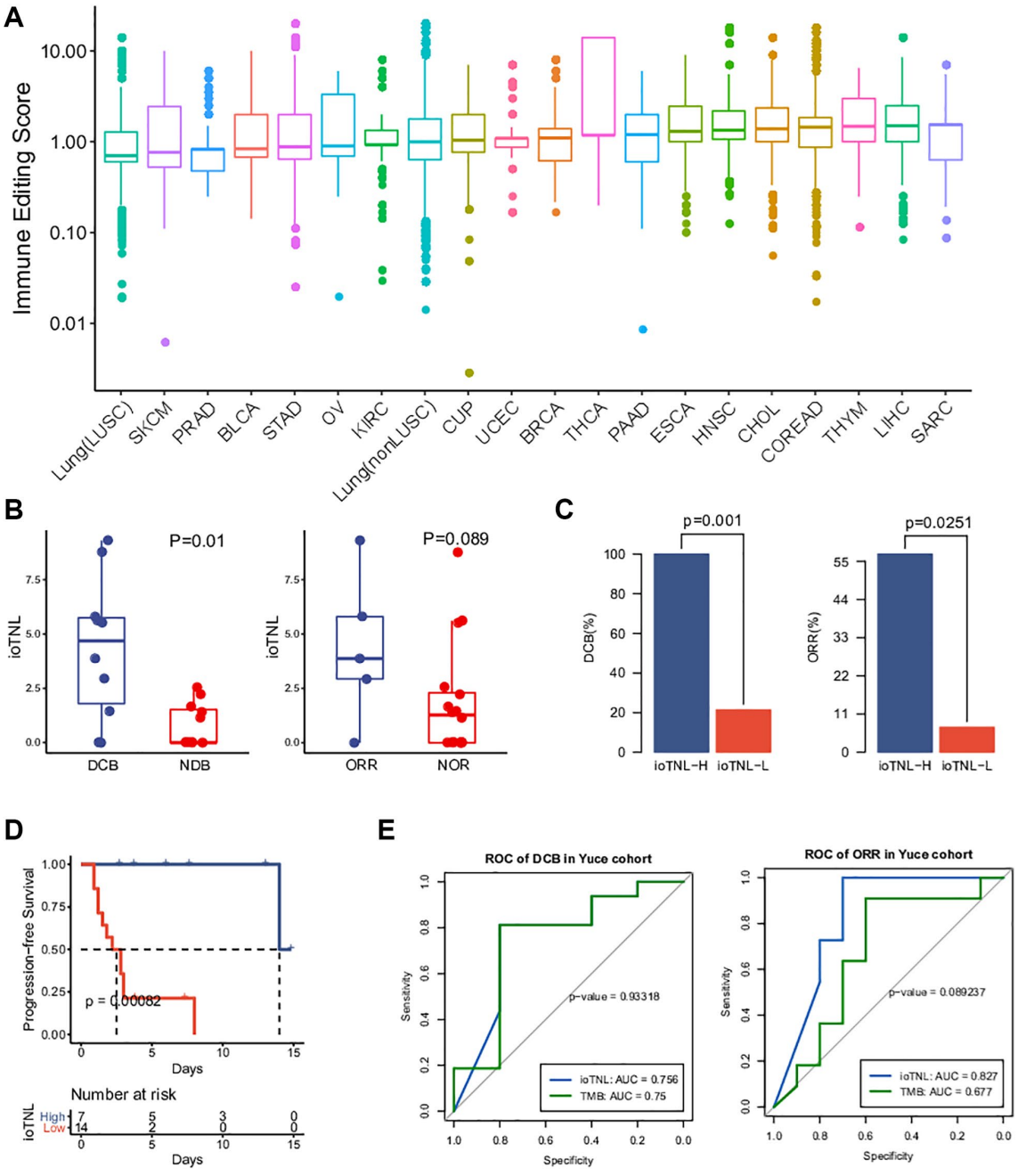

Figure 5. Landscape of immune editing score and application of ioTNL on panel-based Yuce cohort. (**A**) Landscape of immune editing score in 20 cancer types. The immune editing scores were scale in log10 on y-axis. 20 cancer types were label on x-axis and arranged in ascending order by their median immune editing score. (**B**) Boxplots of the distribution of ioTNL scores between patients with DCB and NDB (left), also with ORR and NOR (right). (**C**) Barplots of DCB rate (left) and ORR rate (right) between ioTNL-H group and ioTNL-L group. (**D**) Kaplan-Meier analysis of patient progression-free survival between ioTNL-H group and ioTNL-L group. (**E**) Comparison of sensitivity and specificity between ioTNL and TMB in predicting patient DCB (left) and ORR (right).

DISCUSSION

We developed an algorithm named ioTNL optimised from the tumor neoantigen load based on the immune editing stages. The ioTNL was related to the response and survival in NSCLC, SKCM, melanoma, ICC and NPC. Our data demonstrated that ioTNL could be a prediction model for checkpoint inhibitors, which is more robust than the traditional neoantigen count model and the TMB.

Compared with an assessment of the TMB, relatively few studies have revealed the correlation between the TNL and clinical outcomes. In these studies, the TNL was usually worse than the TMB in predicting clinical efficacy, likely due to the high false-positive rate of neoantigen prediction. Another reason might be that neoantigens are heterogeneous in tumors. The information on neoantigen clones would be ignored by directly counting the number of neoantigens. Some algorithms, such as DAI, focus on identifying neoantigen profiling with high immunogenicity and demonstrate the difference in the predicted affinity for any given wild-type/mutant peptide pair [14]. Similarly, the fitness model selects the neoantigen with the highest immunogenicity from missense derived to determine the sufficient size of a cancer cell population. Some studies have reported that clonal but not subclonal neoantigens are associated with patient survival, such as the clonal neoantigen burden, DAI and CSiN [15]. The studies optimized the neoantigen quantification method based on the quality and clonality; however, they did not consider immune editing during the evolution of the tumor and host immune microenvironment.

Here, we proposed a direction for improvement based on the neoantigen immunoediting stages. If the tumor clone has been immune edited and lost the ability of immune elimination, the possibility of recognising and eliminating these immune tolerant neoantigens will be reduced. Neoantigens in immune edited clones do not contribute to the immunogenicity of tumors. An extensive analysis of a patient with metastatic colorectal cancer during the 11 years of spatiotemporal follow-up showed that the persistent clone had a higher immunoediting score than the eliminated clone [16]. Depletion of neoantigens has been observed in microsatellite instability (MSI) colorectal cancer, known to be sensitive to ICIs [17]. These studies support our hypothesis that tumor clones designated as immunoedited had immune privilege despite the presence of tumor-infiltrating immune cells. Therefore, these clones were resistant to checkpoint inhibitors, and only clones with elimination capability were sensitive to the drugs. Tumor immunoediting influences the intratumoral heterogeneity and shapes clonal evolution.

Additionally, we optimised the algorithm of immunoediting score calculation. A former study reported that the ratio of the neoantigen to non-silent mutation could be calculated to evaluate the immunoediting status [18]. It represents the ratio of the expected to observed immunogenic mutations per non-silent mutation, which is highly dependent on the background mutation reference sets for the expected neoantigen rate. Therefore, we assessed the prediction efficiency with and without reference sets. We found that the model without a reference set demonstrated best practice performance (Supplementary Figure 5). It has been reported that the neoantigens caused by InDels have higher immunogenicity than those from missense mutations [19]. We also considered InDel-derived neoantigens in the ioTNL algorithm, except for missense-derived neoantigens. Another optimisation is that the ioTNL enriches truncal neoantigens by calculating the total cancer cell fraction as the neoantigen concentration instead of the neoantigen load of tumor clones.

Assessment of the ioTNL could be more suitable for clinical application. In one way, the ioTNL is an RNA-independent method. The expression of mutated genes is essential for neoantigen prediction. Some algorithms, such as the fitness model and CSiN, need transcriptome data to determine whether the mutation is expressed. We used TCGA data instead of transcriptome sequencing to predict the expression level of genes. We assessed the prediction performance of the ioTNL model by comparing models with or without RNA sequencing data to evaluate the expression level of the neoantigens in the SKCM cohort. We found that the performance of the algorithm without RNA sequencing data was not inferior to that with RNA sequencing data (Supplementary Figure 6). Obtaining RNA tissue specimens of high quality is a significant challenge in clinical practice, especially for formalin-fixed paraffin-embedded (FFPE) samples. Such optimisation not only improves the convenience but also reduces the sequencing cost to apply the ioTNL. Furthermore, the ioTNL was validated through the multiple genes targeted panel. This panel was designed to capture HLA genes and regions that enrich neoantigens rather than hotspot mutations. The targeted panel was more suitable for clinical application than WES was due to the low specimen input and cost.

There are some limitations to our study. Although we validated the ioTNL in four different cohorts, including the main cancer types for immune checkpoint therapy (NSCLC and SKCM), the scale of the validation cohort remains limited. More cancer types should be covered in the future, not only including cancers with high load neoantigens (i.e., NSCLC and SKCM) but also those

with median load neoantigens (i.e., ICC and NPC). Recent studies revealed that genomic biomarkers such as the TMB failed to predict the clinical outcome of combination immunotherapy. The ioTNL had a better predictive ability than the TMB and TNL in our data. However, the ioTNL needs to be verified as a genomic biomarker for predictive performance in combination immunotherapy, combined with microenvironmental biomarkers, such as PD-L1, IFN-gamma signature and T cell infiltration. Finally, the accurate identification of neoantigens is the supreme challenge for the ioTNL algorithm, which is also a common challenge in the research on neoantigens. We believe the addition of mass spectrometry data would improve the accuracy of identifying the neoantigens by applying artificial intelligence technology.

In conclusion, we developed a neoantigen algorithm based on immune editing to evaluate the response and prognosis of ICIs. We validated the prediction performance of the ioTNL in four cancers, including NSCLC, SKCM, ICC and NPC. The ioTNL predicted the response and prognosis better than the TMB and TNL. The multiple genes targeted panel was developed for ioTNL testing and can be considered to personalise immunotherapy. The immunoediting stages integrated into the ioTNL should also be considered in neoantigen selection for adoptive cell transfer and vaccine development.

METHODS

Mutation calling

After removing the reads containing sequencing adapters and low-quality reads with more than five ambiguous bases, high-quality reads were aligned to the NCBI human reference genome (hg19) using BWA (v0.5.9) [20] with default parameters. Picard (v1.54) [21] (http://picard.sourceforge.net/) was used to mark duplicates, followed by the use of the Genome Analysis Toolkit [22] (v1.0.6076, GATK IndelRealigner) to improve alignment accuracy.

Somatic SNVs were detected by VarScan2.2.5 [23] based on the BWA align algorithm and high-confidence somatic SNVs were called if the following criteria were met: (I) both the tumor and normal samples were covered sufficiently (≥ 10×) at the genomic position; (II) the variants were supported by at least 5% of the total reads in the tumor in contrast to less than 2% in the normal; (III) the variants were supported by at least three reads in the tumor; (IV) the distance between adjacent somatic SNVs were over 10 bp; (V) the mapping qualities of reads supporting the mutant allele in the tumor were significantly higher than 30 (Wilcoxon rank sum test, $P < 0.2$); (VI) the base qualities of reads supporting the mutant allele in the tumor were significantly higher than 20 (Wilcoxon rank sum test, $P < 0.05$); (VII) the mutations were not enriched within the 5 bp 5' or 3' of the read end (Wilcoxon rank sum test, $P < 0.1$); (VIII) the mutant allele frequency changes between the tumor and blood were statistically significant (Fisher's exact test, $P < 0.05$).

High-confidence somatic InDels were called based on the following steps: (I) candidate somatic InDels were predicted with the GATK somatic InDel detector with default parameters; (II) for each predicted somatic InDel, local realignment was performed with combined normal and tumor bam files; (III) frequent of variant reads less than 10% were filtered. (IV) high-confidence somatic InDels were defined after filtering germline events.

Finally, all mutations were re-annotated using in-house annotation software based on SnpEff [24].

Copy number analysis and tumor purity assessment

Copy number variants (CNV) were called by exome-wide profile comparisons between tumors and matched peripheral blood using CNVkit (v0.8.1). Allele-specific copy number and tumor purity of the tumor genome were assessed using ascatNgs (v3.1.0).

HLA class I neoantigen predictions, prioritization, and selection

HLA genotype is identified with combination use of Polysover [25] and BWA-HLA. 9-mer polypeptides centered on mutated residues were scanned to identify candidate peptides binding to HLA class I, i.e., peptide sequences surrounding mutated amino acids resulting from missense mutations, frame-shift or non-frame-shift indels. The affinity of 8–11 mer peptides binding to HLA class I was predicted using the NetMHCPan4.0 [26] binding algorithm.

Tumor clone determination

PyClone (v0.13.0) was used to infer the cancer cell fraction (CCF) of mutations in tumors. Major copy number and minor copy number of each mutation were acquired from the result of ascatNgs software. Moreover, set prior to major_copy_number. For some samples whose copy number of each SNV and tumor purity information were not accessible, those parameters were set to the default value and set prior to total_copy_number. PyClone was deployed with 10,000 iterations and a burn-in of 1000 for all samples.

Calculation of immune editing score and ioTNL score

ioTNL was calculated by counting neoantigen concentration selected from tumor clones which could induce immune elimination. We calculated the ratio of neoantigen to non-silent mutation as immune editing score to quantify the immune editing stages for tumor clones.

$$Immune\ editing\ score = \frac{n_{neoantigen}}{n_{nonsilent\ mutation}}$$

Tumor clonal architecture was calculated by PyClone. Cancer cell fraction of each neoantigen in the immune elimination clone were sum up as final ioTNL.

$$ioTNL = \sum_{i=1}^{n} load_i \times CCF_i$$

Where n represents the total number of immune elimination clone, $load_i$ is the number of neoantigens in the immune elimination clone i and CCF_i is the cancer cell fraction in the immune elimination clone i. We found the best cutoff of immune editing score from 0.5 to 1.5 in increment of 0.1 when the best prediction performance of ioTNL was found. The best prediction performance of ioTNL was found as maximum area of ROC curve. The cutoff of ioTNL was identified by Youden index (the maximum sensitivity and the best specificity under the AUC curve).

Statistical analysis

Categorical variables were evaluated with Fisher's exact tests. Unpaired Mann–Whitney *U* test was used to compare differences for continuous variables between groups. Correlation analysis was assessed by Pearson coefficient. ROC analysis was done using the ROCR package in R. Significance of overall survival (OS) and progression-free survival (PFS) was determined via Kaplan-Meier analysis with log-rank analysis. The hazard ratio was calculated by the coxph function of the survival package in R. All statistical analysis was performed in the R statistical environment version 3.6.1. All tests were two-tailed and p-value < 0.05 was considered significant.

Ethics approval and consent to participate

A 68-year-old squamous cell carcinoma of the lung cancer patient01 was enrolled in Shanghai Tenth People's Hospital on 2018. The study was approved by Shanghai Tenth People's Hospital ethics committee. The patient provided written informed consent.

Availability of data and material

All of the published data used in the article can be found on the NCBI website and supplementary material, all the material used in the experiment can be bought. Codes and YuceOne (panel-based) data are available upon reasonable request.

Abbreviations

ioTNL: immunoediting based optimized neoantigen load; NSCLC: non-small cell lung cancer; SKCM: skin cutaneous melanoma; NPC: nasopharyngeal carcinoma; ICC: intrahepatic cholangiocarcinoma; anti-PD-(L)1: anti-programmed death-(ligand) 1; MHC: major histocompatibility complex; TCR: T-cell receptor; HLA: human leukocyte antigen; InDels: insertions and deletions; ORR: objective response rate; NOR: non-objective response; DCB: durable clinical benefit; NDB: non-durable clinical benefit; CR: complete response; PR: partial response; SD: stable disease; PD: disease progression; PFS: progression-free survival; OS: overall survival; TMB: tumor mutation burden; TNB: tumor neoantigen burden; ROC: receiver operating characteristic curve; AUC: area under curve; CCF: cancer cell fraction.

AUTHOR CONTRIBUTIONS

MXL, XFS and ZBG conceived and designed the study. This manuscript was written by XFS, JQW and HXJ. This model was developed by JQW and HXJ. The validation of the performance of the algorithm was conducted by JQW and HXJ. XFS, HPL and TTG collected clinical information that was used in the study. All authors contributed equally to critically revising the manuscript and providing final approval of the submitted manuscript.

ACKNOWLEDGMENTS

Thanks to Longyun Chen for discussions and suggestions.

CONFLICTS OF INTEREST

The authors declare no conflicts of interest related to this study.

REFERENCES

1. Yarchoan M, Hopkins A, Jaffee EM. Tumor Mutational Burden and Response Rate to PD-1 Inhibition. N Engl J Med. 2017; 377:2500–1. https://doi.org/10.1056/NEJMc1713444 PMID:29262275

2. McGranahan N, Furness AJ, Rosenthal R, Ramskov S, Lyngaa R, Saini SK, Jamal-Hanjani M, Wilson GA, Birkbak NJ, Hiley CT, Watkins TB, Shafi S, Murugaesu N, et al. Clonal neoantigens elicit T cell immunoreactivity and sensitivity to immune checkpoint blockade. Science. 2016; 351:1463–9. https://doi.org/10.1126/science.aaf1490 PMID:26940869

3. Łuksza M, Riaz N, Makarov V, Balachandran VP, Hellmann MD, Solovyov A, Rizvi NA, Merghoub T, Levine AJ, Chan TA, Wolchok JD, Greenbaum BD. A neoantigen fitness model predicts tumour response to checkpoint blockade immunotherapy. Nature. 2017; 551:517–20. https://doi.org/10.1038/nature24473 PMID:29132144

4. Rosenthal R, Cadieux EL, Salgado R, Bakir MA, Moore DA, Hiley CT, Lund T, Tanić M, Reading JL, Joshi K, Henry JY, Ghorani E, Wilson GA, et al, and TRACERx consortium. Neoantigen-directed immune escape in lung cancer evolution. Nature. 2019; 567:479–85. https://doi.org/10.1038/s41586-019-1032-7 PMID:30894752

5. Anagnostou V, Smith KN, Forde PM, Niknafs N, Bhattacharya R, White J, Zhang T, Adleff V, Phallen J, Wali N, Hruban C, Guthrie VB, Rodgers K, et al. Evolution of Neoantigen Landscape during Immune Checkpoint Blockade in Non-Small Cell Lung Cancer. Cancer Discov. 2017; 7:264–76. https://doi.org/10.1158/2159-8290.CD-16-0828 PMID:28031159

6. Nejo T, Matsushita H, Karasaki T, Nomura M, Saito K, Tanaka S, Takayanagi S, Hana T, Takahashi S, Kitagawa Y, Koike T, Kobayashi Y, Nagae G, et al. Reduced Neoantigen Expression Revealed by Longitudinal Multiomics as a Possible Immune Evasion Mechanism in Glioma. Cancer Immunol Res. 2019; 7:1148–61. https://doi.org/10.1158/2326-6066.CIR-18-0599 PMID:31088845

7. Chowell D, Morris LGT, Grigg CM, Weber JK, Samstein RM, Makarov V, Kuo F, Kendall SM, Requena D, Riaz N, Greenbaum B, Carroll J, Garon E, et al. Patient HLA class I genotype influences cancer response to checkpoint blockade immunotherapy. Science. 2018; 359:582–7. https://doi.org/10.1126/science.aao4572 PMID:29217585

8. Montesion M, Murugesan K, Jin DX, Sharaf R, Sanchez N, Guria A, Minker M, Li G, Fisher V, Sokol ES, Pavlick DC, Moore JA, Braly A, et al. Somatic HLA Class I Loss Is a Widespread Mechanism of Immune Evasion Which Refines the Use of Tumor Mutational Burden as a Biomarker of Checkpoint Inhibitor Response. Cancer Discov. 2021; 11:282–92. https://doi.org/10.1158/2159-8290.CD-20-0672 PMID:33127846

9. Roudko V, Bozkus CC, Orfanelli T, McClain CB, Carr C, O'Donnell T, Chakraborty L, Samstein R, Huang KL, Blank SV, Greenbaum B, Bhardwaj N. Shared Immunogenic Poly-Epitope Frameshift Mutations in Microsatellite Unstable Tumors. Cell. 2020; 183:1634–49.e17. https://doi.org/10.1016/j.cell.2020.11.004 PMID:33259803

10. Fang W, Ma Y, Yin JC, Hong S, Zhou H, Wang A, Wang F, Bao H, Wu X, Yang Y, Huang Y, Zhao H, Shao YW, Zhang L. Comprehensive Genomic Profiling Identifies Novel Genetic Predictors of Response to Anti-PD-(L)1 Therapies in Non-Small Cell Lung Cancer. Clin Cancer Res. 2019; 25:5015–26. https://doi.org/10.1158/1078-0432.CCR-19-0585 PMID:31085721

11. Riaz N, Havel JJ, Makarov V, Desrichard A, Urba WJ, Sims JS, Hodi FS, Martín-Algarra S, Mandal R, Sharfman WH, Bhatia S, Hwu WJ, Gajewski TF, et al. Tumor and Microenvironment Evolution during Immunotherapy with Nivolumab. Cell. 2017; 171:934–49.e16. https://doi.org/10.1016/j.cell.2017.09.028 PMID:29033130

12. Feng K, Liu Y, Zhao Y, Yang Q, Dong L, Liu J, Li X, Zhao Z, Mei Q, Han W. Efficacy and biomarker analysis of nivolumab plus gemcitabine and cisplatin in patients with unresectable or metastatic biliary tract cancers: results from a phase II study. J Immunother Cancer. 2020; 8:e000367. https://doi.org/10.1136/jitc-2019-000367 PMID:32487569

13. Fang W, Yang Y, Ma Y, Hong S, Lin L, He X, Xiong J, Li P, Zhao H, Huang Y, Zhang Y, Chen L, Zhou N, et al. Camrelizumab (SHR-1210) alone or in combination with gemcitabine plus cisplatin for nasopharyngeal carcinoma: results from two single-arm, phase 1 trials. Lancet Oncol. 2018; 19:1338–50. https://doi.org/10.1016/S1470-2045(18)30495-9 PMID:30213452

14. Ghorani E, Rosenthal R, McGranahan N, Reading JL, Lynch M, Peggs KS, Swanton C, Quezada SA. Differential binding affinity of mutated peptides for MHC class I is a predictor of survival in advanced lung cancer and melanoma. Ann Oncol. 2018; 29:271–9. https://doi.org/10.1093/annonc/mdx687 PMID:29361136

15. Lu T, Wang S, Xu L, Zhou Q, Singla N, Gao J, Manna S, Pop L, Xie Z, Chen M, Luke JJ, Brugarolas J, Hannan R, Wang T. Tumor neoantigenicity assessment with CSiN score incorporates clonality and immunogenicity to

predict immunotherapy outcomes. Sci Immunol. 2020; 5:eaaz3199.
https://doi.org/10.1126/sciimmunol.aaz3199
PMID:32086382

16. Angelova M, Mlecnik B, Vasaturo A, Bindea G, Fredriksen T, Lafontaine L, Buttard B, Morgand E, Bruni D, Jouret-Mourin A, Hubert C, Kartheuser A, Humblet Y, et al. Evolution of Metastases in Space and Time under Immune Selection. Cell. 2018; 175:751–65.e16.
https://doi.org/10.1016/j.cell.2018.09.018
PMID:30318143

17. Mlecnik B, Bindea G, Angell HK, Maby P, Angelova M, Tougeron D, Church SE, Lafontaine L, Fischer M, Fredriksen T, Sasso M, Bilocq AM, Kirilovsky A, et al. Integrative Analyses of Colorectal Cancer Show Immunoscore Is a Stronger Predictor of Patient Survival Than Microsatellite Instability. Immunity. 2016; 44:698–711.
https://doi.org/10.1016/j.immuni.2016.02.025
PMID:26982367

18. Rooney MS, Shukla SA, Wu CJ, Getz G, Hacohen N. Molecular and genetic properties of tumors associated with local immune cytolytic activity. Cell. 2015; 160:48–61.
https://doi.org/10.1016/j.cell.2014.12.033
PMID:25594174

19. Turajlic S, Litchfield K, Xu H, Rosenthal R, McGranahan N, Reading JL, Wong YNS, Rowan A, Kanu N, Al Bakir M, Chambers T, Salgado R, Savas P, et al. Insertion-and-deletion-derived tumour-specific neoantigens and the immunogenic phenotype: a pan-cancer analysis. Lancet Oncol. 2017; 18:1009–21.
https://doi.org/10.1016/S1470-2045(17)30516-8
PMID:28694034

20. Li H, Durbin R. Fast and accurate short read alignment with Burrows-Wheeler transform. Bioinformatics. 2009; 25:1754–60.
https://doi.org/10.1093/bioinformatics/btp324
PMID:19451168

21. Picard. 2013. http://picard.sourceforge.net/

22. McKenna A, Hanna M, Banks E, Sivachenko A, Cibulskis K, Kernytsky A, Garimella K, Altshuler D, Gabriel S, Daly M, DePristo MA. The Genome Analysis Toolkit: a MapReduce framework for analyzing next-generation DNA sequencing data. Genome Res. 2010; 20:1297–303.
https://doi.org/10.1101/gr.107524.110
PMID:20644199

23. Koboldt DC, Zhang Q, Larson DE, Shen D, McLellan MD, Lin L, Miller CA, Mardis ER, Ding L, Wilson RK. VarScan 2: somatic mutation and copy number alteration discovery in cancer by exome sequencing. Genome Res. 2012; 22:568–76.
https://doi.org/10.1101/gr.129684.111
PMID:22300766

24. Cingolani P, Platts A, Wang le L, Coon M, Nguyen T, Wang L, Land SJ, Lu X, Ruden DM. A program for annotating and predicting the effects of single nucleotide polymorphisms, SnpEff: SNPs in the genome of Drosophila melanogaster strain w1118; iso-2; iso-3. Fly (Austin). 2012; 6:80–92.
https://doi.org/10.4161/fly.19695
PMID:22728672

25. Shukla SA, Rooney MS, Rajasagi M, Tiao G, Dixon PM, Lawrence MS, Stevens J, Lane WJ, Dellagatta JL, Steelman S, Sougnez C, Cibulskis K, Kiezun A, et al. Comprehensive analysis of cancer-associated somatic mutations in class I HLA genes. Nat Biotechnol. 2015; 33:1152–8.
https://doi.org/10.1038/nbt.3344
PMID:26372948

26. Jurtz V, Paul S, Andreatta M, Marcatili P, Peters B, Nielsen M. NetMHCpan-4.0: Improved Peptide-MHC Class I Interaction Predictions Integrating Eluted Ligand and Peptide Binding Affinity Data. J Immunol. 2017; 199:3360–8.
https://doi.org/10.4049/jimmunol.1700893
PMID:28978689

SUPPLEMENTARY MATERIALS

Supplementary Figures

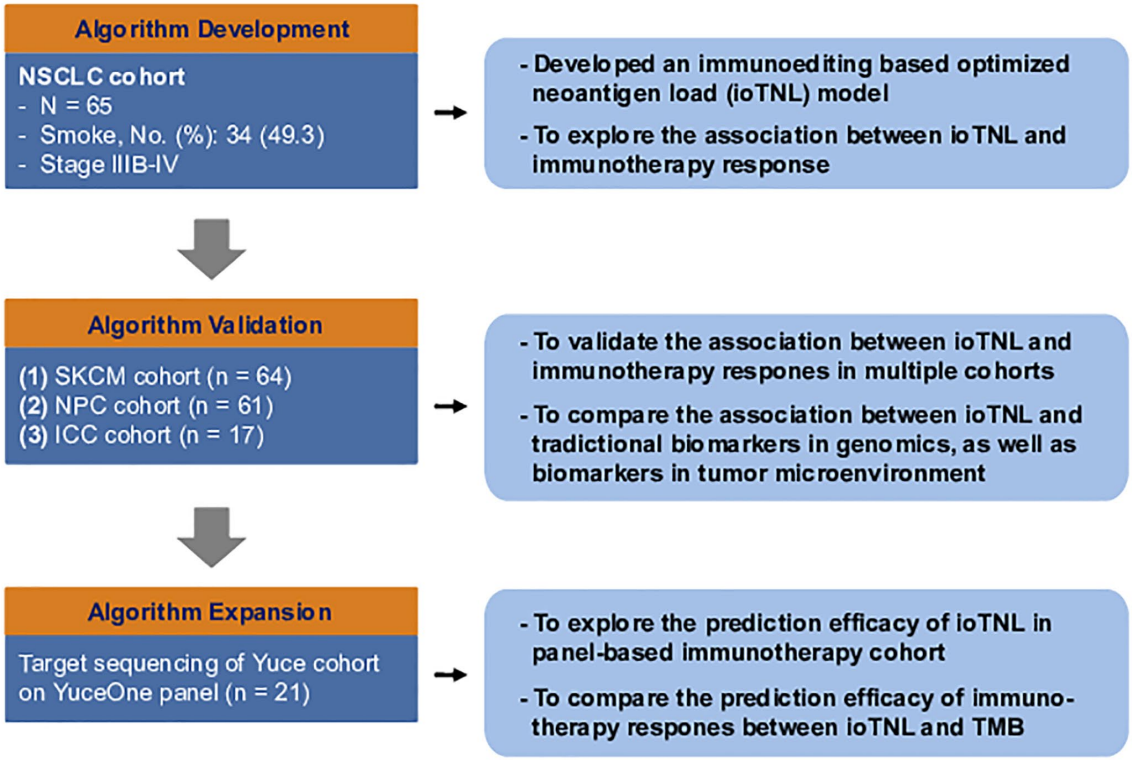

Supplementary Figure 1. The study diagram of the ioTNL model.

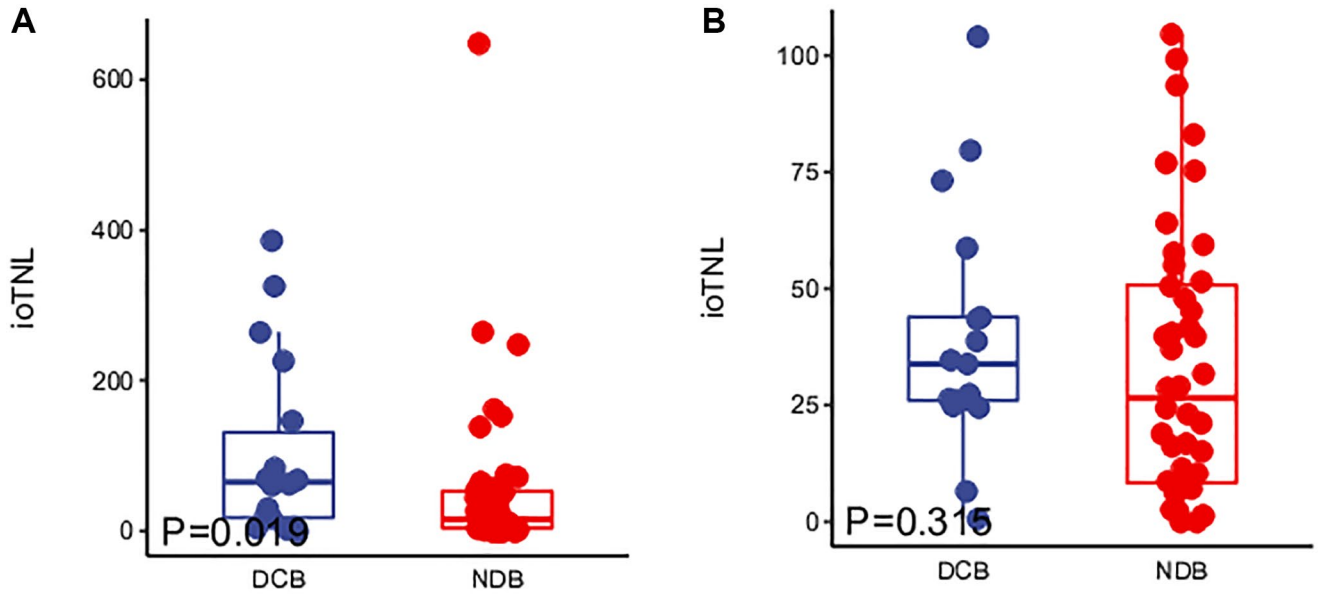

Supplementary Figure 2. Boxplots of the distribution of ioTNL scores between patients with DCB and NDB in the NSCLC cohort (**A**) and the NPC cohort (**B**).

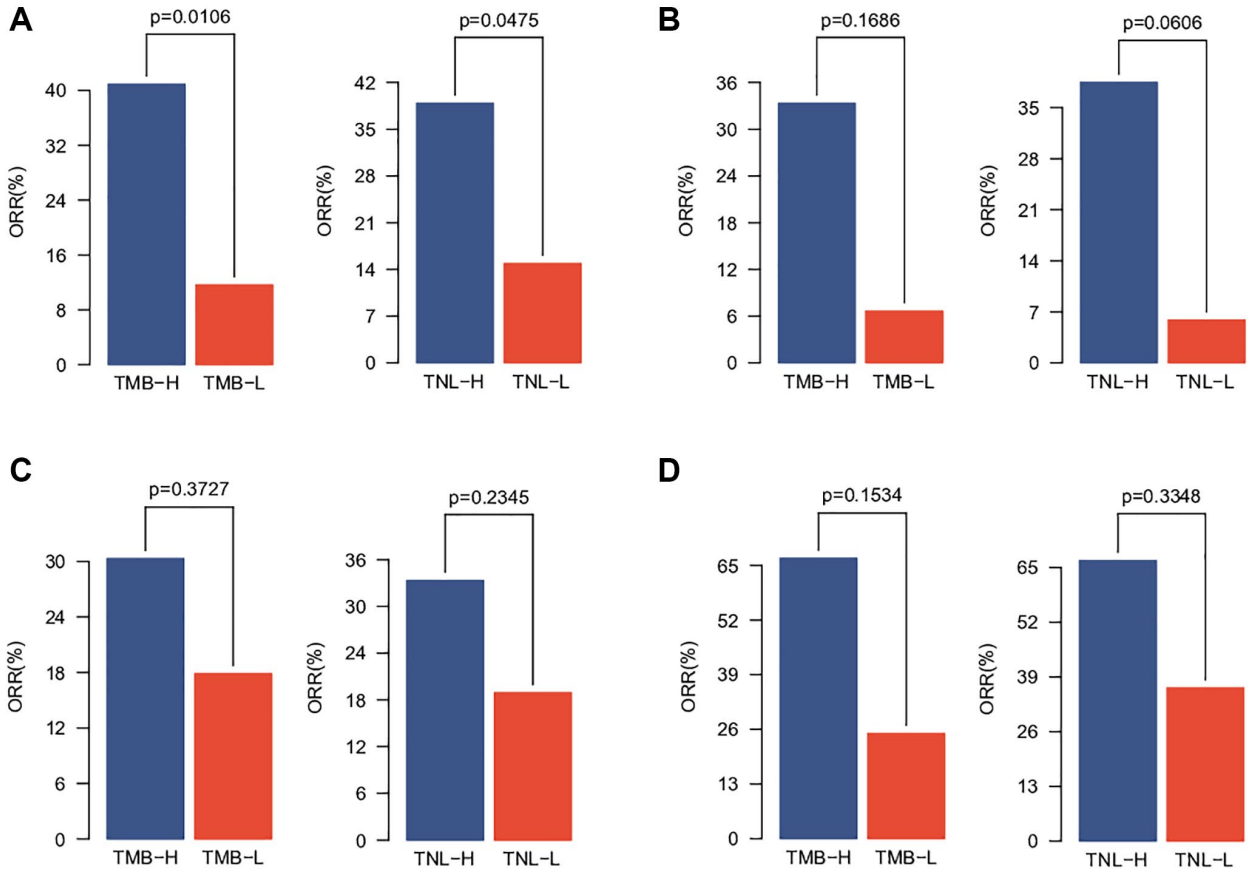

Supplementary Figure 3. Barplots of ORR rate of different TMB levels and TNL levels in the NSCLC cohort (**A**), the SKCM cohort (**B**), the NPC cohort (**C**) and the ICC cohort (**D**).

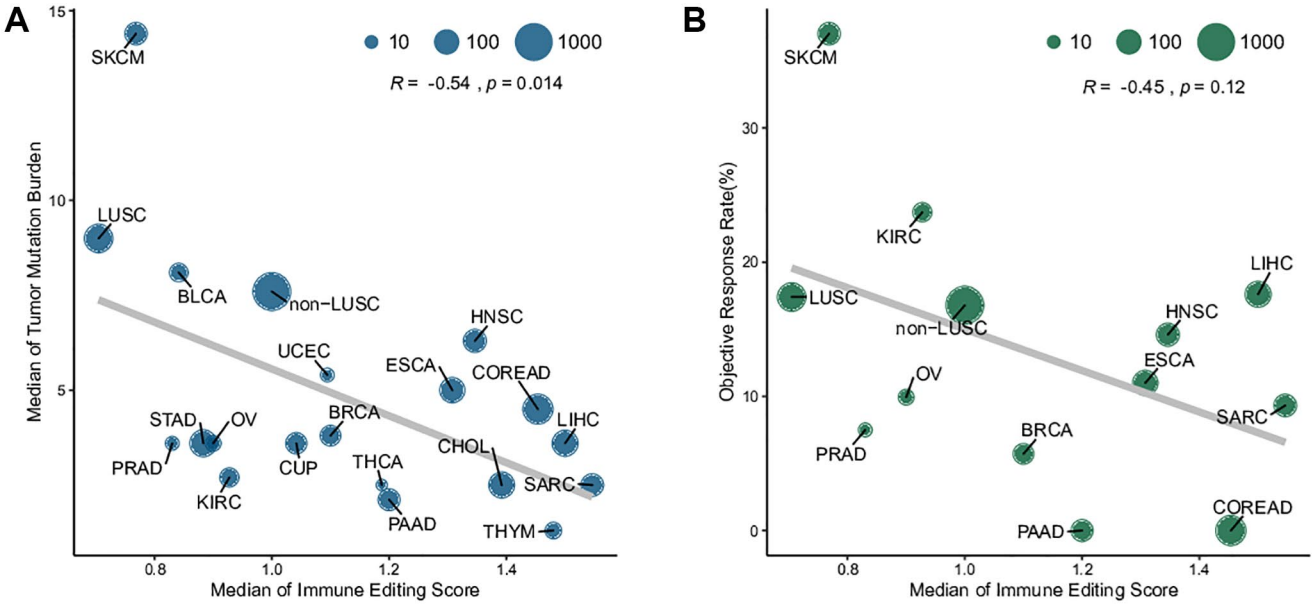

Supplementary Figure 4. Immune editing score was associated with TMB and objective response rate of immunotherapy. (**A**) Correlation between median immune editing score and median TMB in 20 cancer types. (**B**) Correlation between median immune editing score and objective response rate of immunotherapy in multiple cancer types. Size of circle represents the number of patients that involved in the evaluation of immune editing score.

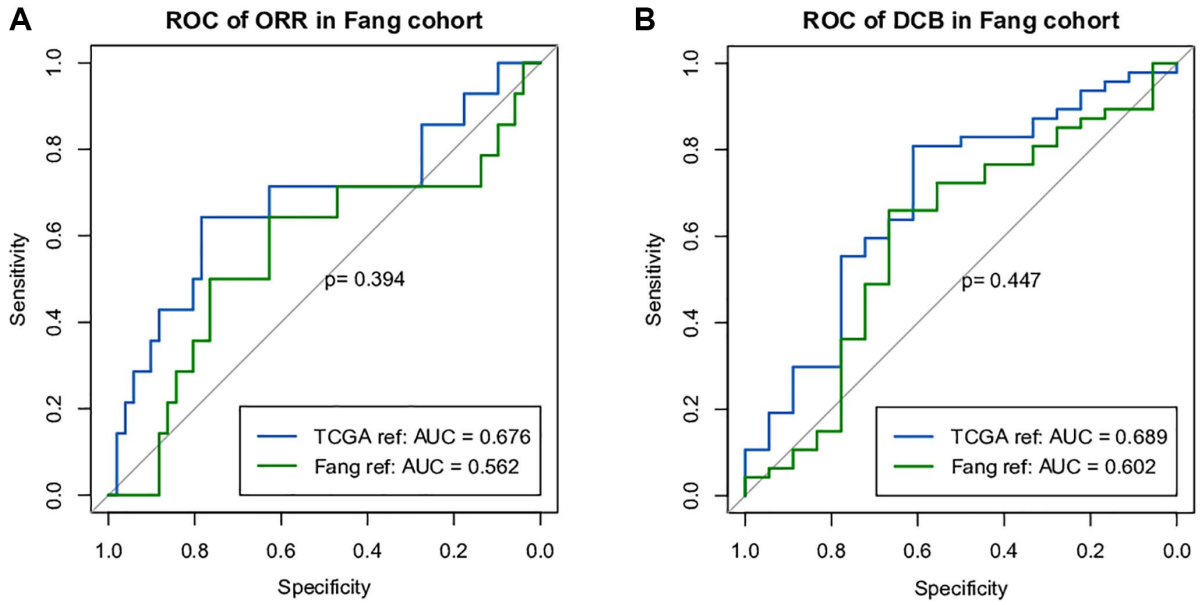

Supplementary Figure 5. Prediction efficiency with different reference set of ORR (**A**) and DCB (**B**) in the NSCLC cohort.

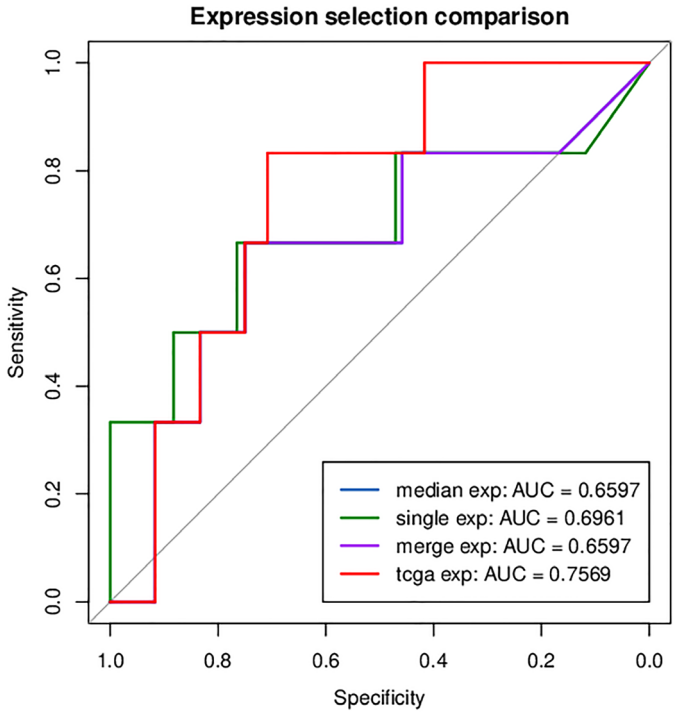

Supplementary Figure 6. Prediction efficiency with different gene expression dataset.

Supplementary Tables

Supplementary Table 1. Detailed information of the introduced immunotherapy cohorts.

Cohort	Cohort size	Histology	Treatment	Sequence type	References
NSCLC cohort	65	Non-small-cell lung cancer	Anti-PD-(L)1	WES	Fang et al., 2019
SKCM cohort	64	Skin cutaneous melanoma	Anti-PD-1	WES	Riaz et al., 2017
NPC cohort	61	Nasopharyngeal carcinoma	Anti-PD-(L)1	WES	Fang et al., 2018
ICC cohort	17	Intrahepatic cholangiocarcinoma	Anti-PD-1 + chemotherapy	WES	Feng et al., 2020
Yuce cohort	21	Non-small-cell lung cancer	Anti-PD-1	Panel	–
Total	228				

Please browse Full Text version to see the data of Supplementary Tables 2, 4 and 6.

Supplementary Table 2. Summary of ioTNL and clinical characteristics in NSCLC cohort.

Supplementary Table 3. Summary of ioTNL and clinical characteristics in SKCM cohort.

Patient	Sample	TMB	TNL	ioTNL	Treated	Response	ORR	OS	Status
PT100	PT100-BE	0.13	0.1	0	NIV3-PROG	PD	NOR	120	1
PT101	PT101-BE	0.1	0.07	0	NIV3-PROG	PR	ORR	119.1	0
PT103	PT103-BE	0.26	0.19	0	NIV3-PROG	PD	NOR	69.1	0
PT104	PT104-BE	0.16	0.1	0	NIV3-PROG	PR	ORR	116.9	0
PT106	PT106-BE	18.59	7.89	340.327	NIV3-PROG	PD	NOR	13	1
PT108	PT108-BE	0.62	0.16	3.098	NIV3-PROG	SD	NOR	130.4	0
PT10	PT10-BE	2.48	0.89	28.9125	NIV3-NAIVE	SD	NOR	36.6	1
PT11	PT11-BE	2.3	1.26	47.0899	NIV3-NAIVE	PD	NOR	119.6	1
PT13	PT13-BE	4.48	2.08	82.1663	NIV3-NAIVE	PD	NOR	40	1
PT17	PT17-BE	0.16	0.16	0	NIV3-PROG	PD	NOR	8.1	1
PT18	PT18-BE	4.31	2.5	92.5359	NIV3-NAIVE	PR	ORR	153.3	0
PT24	PT24-BE	0.1	0.03	0	NIV3-NAIVE	PD	NOR	21.3	0
PT25	PT25-BE	2.27	1.36	0	NIV3-NAIVE	PD	NOR	14.4	1
PT27	PT27-BE	4.69	2.88	0	NIV3-NAIVE	PD	NOR	67.9	1
PT28	PT28-BE	1.2	0.68	7.0901	NIV3-NAIVE	PD	NOR	105.7	1
PT29	PT29-BE	11.54	7.17	0.5179	NIV3-NAIVE	PD	NOR	39	1
PT30	PT30-BE	1.82	0.42	18.1944	NIV3-NAIVE	CR	ORR	150.4	0
PT31	PT31-BE	10.86	5.48	166.906	NIV3-NAIVE	PD	NOR	137.3	0
PT32	PT32-BE	3.2	1.45	56.7156	NIV3-PROG	PD	NOR	16.3	0
PT34	PT34-BE	3.77	2.63	107.228	NIV3-PROG	PR	ORR	119.1	0
PT36	PT36-BE	0.19	0.1	0	NIV3-PROG	SD	NOR	154.4	0
PT37	PT37-BE	0.57	0.27	3.73814	NIV3-PROG	SD	NOR	92.3	1
PT38	PT38-BE	9.4	4.56	94.1405	NIV3-PROG	SD	NOR	23.9	1

PT3	PT3-BE	4.93	2.24	98.4519	NIV3-NAIVE	PR	ORR	163.4	0
PT44	PT44-BE	10.39	4.88	274.331	NIV3-NAIVE	PR	ORR	156.1	0
PT46	PT46-BE	4.02	2.43	0	NIV3-PROG	PD	NOR	32.4	1
PT47	PT47-BE	24.8	12.64	535.166	NIV3-PROG	PD	NOR	102.6	1
PT48	PT48-BE	1.83	0.93	21.0797	NIV3-PROG	CR	ORR	149.4	0
PT4	PT4-BE	6.9	1.78	97.4983	NIV3-NAIVE	SD	NOR	90.4	1
PT51	PT51-BE	5.91	2.5	93.7713	NIV3-PROG	PD	NOR	8.1	0
PT52	PT52-BE	7.68	4	130.458	NIV3-PROG	PD	NOR	68	1
PT53	PT53-BE	2.08	0.52	14.6259	NIV3-PROG	PR	ORR	61.9	1
PT58	PT58-BE	22.65	10.97	524.13	NIV3-PROG	SD	NOR	71.3	1
PT59	PT59-BE	9.58	3.77	127.405	NIV3-NAIVE	SD	NOR	101.1	1
PT5	PT5-BE	0.85	0.36	6.06482	NIV3-NAIVE	PD	NOR	31.7	1
PT60	PT60-BE	17.36	8.07	451.967	NIV3-NAIVE	PD	NOR	105.4	0
PT66	PT66-BE	3.94	1.7	72.4464	NIV3-NAIVE	PD	NOR	77.4	1
PT67	PT67-BE	0.45	0.26	0	NIV3-PROG	SD	NOR	147.4	0
PT68	PT68-BE	19.34	9.46	382.127	NIV3-PROG	PR	ORR	120.3	0
PT70	PT70-BE	11.3	7.72	417.55	NIV3-PROG	SD	NOR	44.4	1
PT71	PT71-BE	0.35	0.13	0	NIV3-NAIVE	SD	NOR	35.1	0
PT72	PT72-BE	12.11	5.76	262.428	NIV3-NAIVE	PR	ORR	110	1
PT73	PT73-BE	0.45	0.1	1.02686	NIV3-NAIVE	SD	NOR	40.1	0
PT74	PT74-BE	1.48	0.75	32.3266	NIV3-NAIVE	NE	NOR	2.9	1
PT76	PT76-BE	6.55	3.21	124.572	NIV3-NAIVE	NE	NOR	1.4	1
PT77	PT77-BE	1.11	0.49	6.35038	NIV3-NAIVE	SD	NOR	67.3	1
PT79	PT79-BE	15.62	8.46	409.153	NIV3-PROG	SD	NOR	31.1	1
PT82	PT82-BE	1.19	0.42	17.9164	NIV3-PROG	SD	NOR	61.3	1
PT83	PT83-BE	8.3	2.51	79.4521	NIV3-PROG	SD	NOR	66	0
PT84	PT84-BE	0.57	0.37	2.72251	NIV3-NAIVE	PD	NOR	21.6	1
PT85	PT85-BE	3.45	1.74	98.2943	NIV3-PROG	PD	NOR	129.1	0
PT86	PT86-BE	14.85	8.33	353.337	NIV3-PROG	PD	NOR	38.9	1
PT87	PT87-BE	17.14	8.34	383.341	NIV3-NAIVE	SD	NOR	139.1	0
PT89	PT89-BE	4.81	1.77	83.7375	NIV3-NAIVE	SD	NOR	120.6	1
PT8	PT8-BE	2.38	1.02	54.6892	NIV3-NAIVE	PD	NOR	37	1
PT90	PT90-BE	8.72	4.33	132.597	NIV3-PROG	PD	NOR	24.9	1
PT92	PT92-BE	16.27	6.78	225.266	NIV3-PROG	SD	NOR	47.6	1
PT93	PT93-BE	0.81	0.46	11.4005	NIV3-PROG	PD	NOR	121.3	0
PT94	PT94-BE	9.19	4.93	141.264	NIV3-NAIVE	CR	ORR	140.1	0
PT98	PT98-BE	0.59	0.33	10.0383	NIV3-PROG	SD	NOR	106.7	1
PT9	PT9-BE	11.13	3.88	166.344	NIV3-NAIVE	PD	NOR	13.1	1

Supplementary Table 4. Summary of ioTNL and clinical characteristics in NPC cohort.

Supplementary Table 5. Summary of ioTNL and clinical characteristics in ICC cohort.

Sample	TMB	TNL	ioTNL	Response	ORR	OS	OS.Status	PFS	PFS.Status
ICC001	2.85	1.39	69.4077	PR	ORR	334	0	NA	0
ICC002	2.96	1.12	37.032	PR	ORR	151	1	114	1
ICC003	1.33	0.65	14.3812	SD	NOR	415	1	236	1
ICC004	4.65	2.03	80.6436	CR	ORR	572	0	324	1
ICC005	4.5	1.5	50.0041	SD	NOR	154	1	86	1
ICC006	2.56	1.37	14.8543	SD	NOR	143	1	129	1
ICC007	3.24	1.36	48.5457	PD	NOR	138	1	45	1
ICC008	0.94	0.25	1.94014	SD	NOR	277	1	172	1
ICC009	1.91	0.5	4.8922	SD	NOR	353	1	230	1
ICC010	1.46	0.94	9.91282	PD	NOR	136	1	66	1
ICC011	3.37	1.63	57.3618	PR	ORR	165	1	82	1
ICC012	1.63	0.53	17.841	PR	ORR	285	1	NA	0
ICC013	6.28	2.24	82.7309	PR	ORR	420	0	NA	0
ICC014	4.46	2.26	74.1739	SD	NOR	251	1	144	1
ICC015	1.39	0.97	0	PR	ORR	190	1	92	1
ICC016	1.3	0.68	0.29386	SD	NOR	49	1	47	1
ICC017	2.94	1.23	36.0288	PR	ORR	129	1	117	1

Supplementary Table 6. Details of predicted neoantigens and corresponded mutations information in pancancer by YuceOne panel.

Supplementary Table 7. Median immune editing score and corresponded median TMB and ORR of immunotherapy in pancancer.

OncoTree	Median Immune Editing Score	Median TMB	ORR	# of Patients
BLCA	0.841269841	8.1	NA	28
BRCA	1.1	3.8	5.7149	41
CHOL	1.391891892	2.5	NA	114
COREAD	1.453608247	4.5	0	254
CUP	1.041666667	3.6	NA	46
ESCA	1.307692308	5	11	99
HNSC	1.346153846	6.3	14.5987	65
KIRC	0.927536232	2.7	23.7273	31
LIHC	1.5	3.6	17.6074	115
LUSC	0.704545455	9	17.402	186
non-LUSC	1	7.6	16.7981	1116
OV	0.9	3.6	9.93794	16
PAAD	1.2	2.112786	0.0006	52
PRAD	0.830188679	3.6	7.49976	11
SARC	1.546391753	2.5	9.32155	60

SKCM	0.768421053	14.4	37.039	58
STAD	0.883116883	3.6	NA	140
THCA	1.1875	2.5	NA	7
THYM	1.48	1.3	NA	19
UCEC	1.094594595	5.4	NA	11

Supplementary Table 8. Summary of ioTNL and clinical characteristics in Yuce cohort.

Sample	TMB	ioTNL	Benefit	DCB	ORR	PFS	Status
Yuce001	3.36	0	PD	NDB	DOR	0.9	1
Yuce002	8.73	0	PD	NDB	DOR	2.2	1
Yuce003	16.13	0	PD	NDB	DOR	1.2	1
Yuce004	12.76	5.60849	SD	DCB	DOR	7.6	0
Yuce005	5.38	0	PD	NDB	DOR	2.8	1
Yuce006	18.13	9.29958	PR	DCB	ORR	3.7	0
Yuce007	8.06	1.15252	PD	NDB	DOR	1.2	1
Yuce008	1.34	0	SD	DCB	DOR	7.3	0
Yuce009	2.02	1.39332	PD	NDB	DOR	0.9	1
Yuce010	6.72	8.75306	SD	DCB	DOR	14	1
Yuce011	15.4	3.86614	PR	DCB	ORR	2.7	0
Yuce012	12.07	5.79855	CR	DCB	ORR	6	0
Yuce013	11.27	2.93277	CR	DCB	ORR	14.8	0
Yuce014	4.65	1.43219	SD	DCB	DOR	8	1
Yuce015	9.96	0	PD	NDB	DOR	3	1
Yuce016	6.64	1.64018	PD	NDB	DOR	2.8	1
Yuce017	12.61	5.50955	SD	DCB	DOR	13	0
Yuce018	1.34	0	PD	NDB	DOR	1.5	1
Yuce019	3.35	0	PR	DCB	ORR	3.8	0
Yuce020	4.02	2.21275	PD	NDB	DOR	3	1
Yuce021	5.36	2.54265	PD	NDB	DOR	1.8	1